Chapter 12

Calcium Ferrit Generation During Iron Ore Sintering — Crystallization Behavior and Influencing Factors

Min Gan, Xiaohui Fan and Xuling Chen

Additional information is available at the end of the chapter

http://dx.doi.org/10.5772/59659

1. Introduction

Iron ore sintering is a heat treatment process for agglomerating fine particles into larger lumps, which then serve as the major burden for blast furnace. The production of high-quality sinter is critical for efficient blast furnace operation [1-3].

Sintering is a complex process involving, as it does, many interrelated physico-chemical phenomena pertaining to flow of gas through the bed of packed granules, heat transfer between gas and solids, chemical reactions between components of the sinter feed and between solid components and gas, etc. Mineralization reaction mainly occurs in preheating layer, combustion layer and initial cooling layer during the sintering process, which is reflected by the ability of solid-phase reactions, the capacity for the generation of liquid phase and the behavior of condensation and crystallization [4,5].

Crystalline condensation is the significant stage of mineralization during iron ore sintering, including the processes that crystalline substance and amorphous substance precipitate from high temperature solution phase, and material is consolidated when melt cooling down. Binder phase of calcium ferrite and part of iron oxides crystallize in this process, which have an important influence on mineral composition and microstructure of sinter, finally determine the sinter strength and metallurgical properties [6-9].

Calcium ferrite has special features such as good intensity, excellent reducibility and low formation temperature, which is suitable for developing low-temperature sintering, improving the qualities of sinter and reducing energy consumption. Crystalline condensation is a key stage to the forming and developing of calcium ferrite, which directly affects its precipitation behavior and crystalline morphology [10-16]. In the paper, the microstructure characteristics of sinter are analyzed, and crystalline condensation mechanism of calcium ferrite binder phase

system based on minerals' precipitation behavior and crystallization condition are studied, also the major factors influencing the generation of calcium ferrite are discussed, which provide theoretical support on improving microstructure of sinter and optimizing its quality.

2. Materials and methods

2.1. Properties of materials

The chemical compositions of raw material for mini-sintering are summarized in Table 1. This mineral, which belongs to oxidized ore, has high iron grade, low gangue content, and the ratio of Total Iron (TFe) to FeO is much higher than 3.5. The chemical, flux (calcium oxide), and the additive (Al_2O_3, SiO_2), is analytic grade reagent.

Raw material	TFe	FeO	CaO	MgO	SiO_2	Al_2O_3	LOI
Iron ore	64.94	0.86	0.03	0.01	3.78	0.77	1.67

Table 1. The chemical compositions of raw material wt/%

2.2. Methods for mini-sintering

Mini-sintering test was used to research the mineralization reactions, such as liquid generation, crystallization behaviour, ect., under high temperature. Horizontal heating furnace whose temperature and atmosphere could be controlled by program was adopted to conduct mini-sintering experiment. The device of mini-sintering was shown in Fig.1.

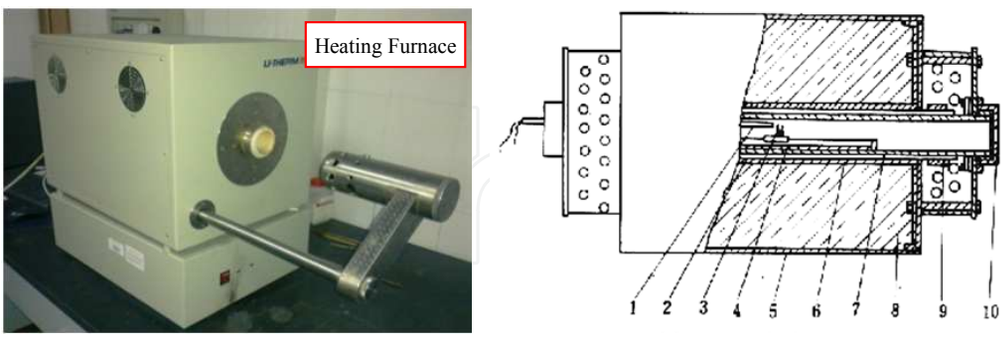

1—thermocouple；2—Silicon tube；3—standard pyrometric cone；4—corundum porcelain boat to load the cone； 5—furnace shell；6—outer thimble of corundum；7—inner sleeve of corundum；8—insulating brick of bubble alumina；9—panel piece；10—peep door

Figure 1. The device of mini-sinter test

In order to simulate sintering process exactly, this experiment divided sintering process into preheating belt, reaction belt, melt belt, solidification belt and sintered belt. On the basis of

http://dx.doi.org/10.5772/59659

physicochemical characteristics of each belt and the actual temperature curve of sintering bed, the heating program and atmosphere simulated were shown in Table.2.

	Temperature/℃	Heating up time /min	Atmosphere
Preheating belt	60 → 700	1	N_2
Reaction belt	700 → 1200	1	$CO:O_2:CO_2$=1:1:5
Melt belt	1200 → 1300	With rate the of 10℃/min	$CO:O_2:CO_2$=1:1:5
Solidification belt	1300 → 1000	2	Air
Sintered belt	1000 → 700	1	Air

Table 2. The heating program and atmosphere of mini-sintering

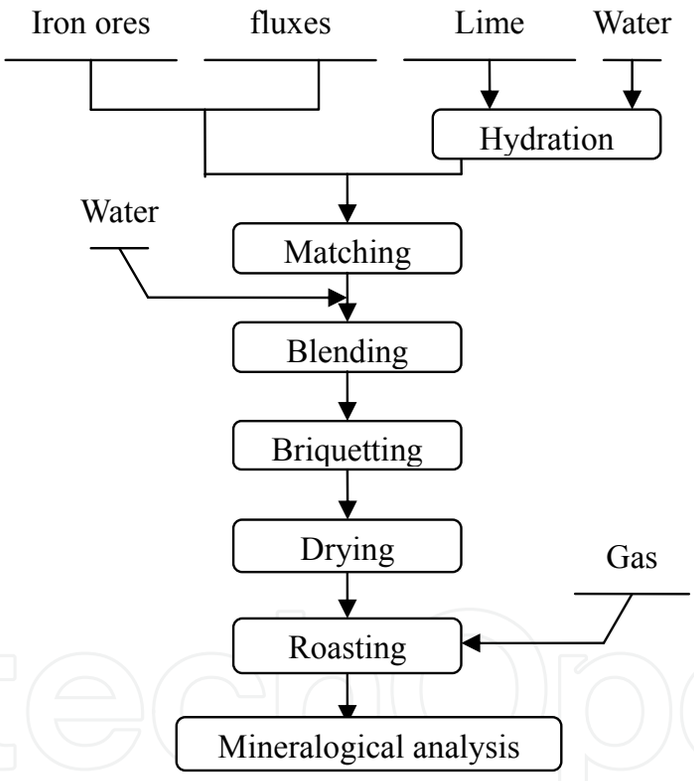

Figure 2. Experimental flow of mini-sintering

The research regarding the formation behavior of SFCA ((Quaternary compound of calcium ferrite containing silicate and alumina) was adopted mini-sinter. The steps of testing mineralization were agglomeration, roasting and mineralogical analysis. The experimental flow is shown in Fig.2.

After ore blended, the mixture was compacted into a cylinder with the size of Φ30×25mm under the pressure of 300kg/cm^2 for 1 min. Then the cylinders were sintered at 1280~1300℃ according

to the heating programs in Table.1. The sintered sample was used to observe the mineralization of sintering mixture. The agglomerates were mounted with epoxy resin, and then polished to form a section, which the microstructures were observed by optical microscope and SEM, and mineral components were detected by image analysis software.

Columnar&acicular SFCA was defined as the ratio of length-diameter was bigger than 2.5. The graphic processing software could recognize the SFCA and figure out its content. The process consisted of image reading, image filtering, identification and segmentation, length-diameter ratio detection, and statistics of selected area.

2.3. Sinter pot test

A 700 mm deep×Φ 180 mm sinter pot was utilised to simulate sintering process, and its schematic diagram was demonstrated in Fig.3.

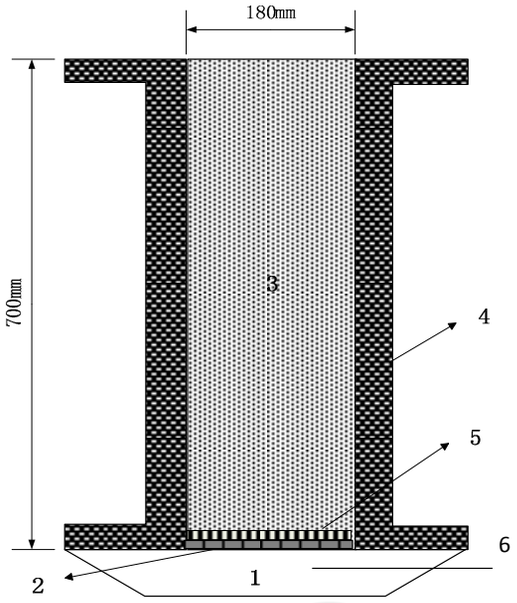

1 vacuum chamber; 2 refracory grate; 3 mixed raw materials;
4 stainless sinter pot; 5 hearth layer;6 thermocouple

Figure 3. Schematic diagram of laboratory sinter pot

Raw materials having been blended and granulated were charged into the sinter pot. Under the mixtures, a hearth layer of approximate 20mm thick was previously prepared to protect the grate from thermal erosion. After charging, the fuel in the surface layer was ignited by an ignition hood initially, and then the combustion front moved downwards with the support of downdraught system, which was mainly a draught fan used to enable sufficient air to be sucked into sinter pot from top.

Apart from that, sintering speed, yield, tumbler index, productivity etc. were detected to evaluate sinter quality. Sintering speed was the ratio of layer height and sintering time, and

http://dx.doi.org/10.5772/59659

yield was the percentage of sinter above 5mm after screening. Productivity reflected the quantity of sinter produced unit area and unit time. Tumbler index, which could reflect sinter strength, was the percentage of sinter above 6.3mm after 7.5kg sinter was tested in a Φ1000×500mm tumbler for 200r.

3. Formation characteristics of calcium ferrite

3.1. Mineralization model for sintering

The mineralization behavior of sintering mixtures in different temperature has been researched, as is shown in Fig.4. When the temperature is at 1100-1150℃, solid-phase reaction occurs, but it was not obvious because of the slow reaction speed. Then when the temperature increases to 1200℃, a large number of CF generate by solid-phase reactions. As the temperature reaches to 1225-1250℃, the liquid phase generates obviously and the holes begin to shrink. Liquid content is developed when the temperature increases to 1300℃. At the temperature of 1300℃, the main mineral constituents are CF, secondary magnetite and hematite.

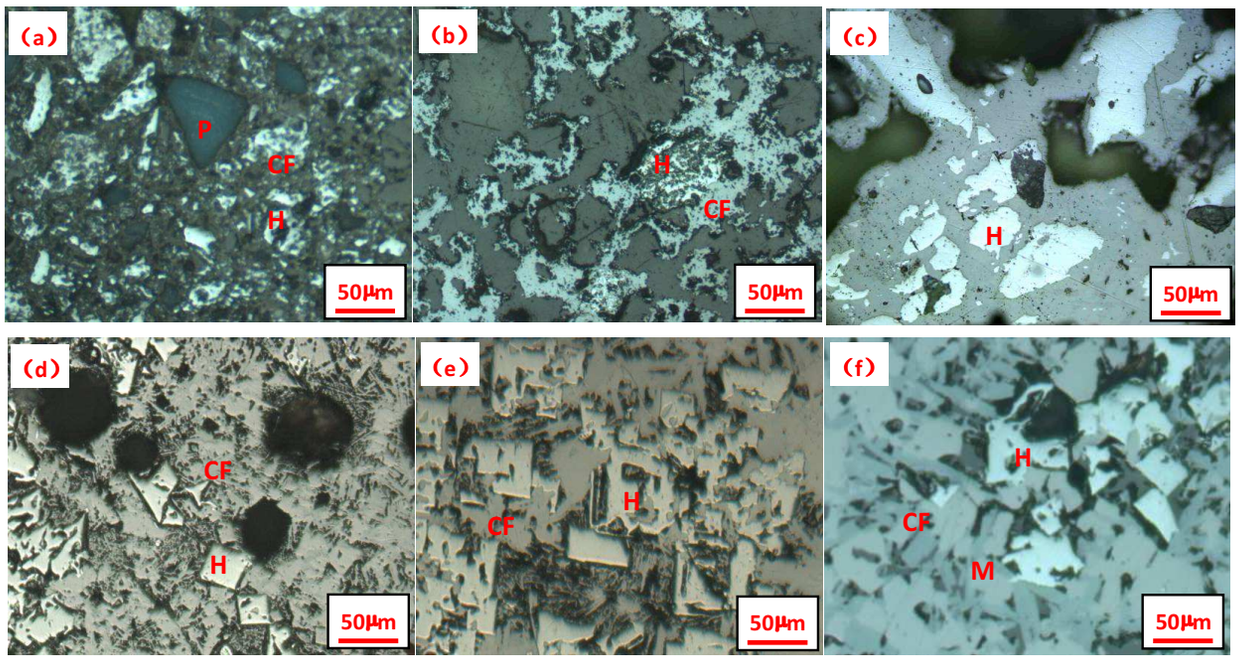

（a）1100℃；（b)1150℃；（c）1200℃；（d）1225℃；（e）1250℃；（f）1300℃

H—hematite，M—magnetite，CF—calcium ferrite，P—pole

Figure 4. Effect of temperature on mineralization of mixture

So, with the increase of the temperature during sintering, reactions occur between fine particles of iron ores and fluxes to form low-melting compounds and then generate liquid phase, but iron ore nuclei almost would not participate in the reaction for its low reacting speed. As the

temperature rises continually, the amount of liquid phase is increased and the fluidity of liquid improved. In the process of temperature-fall, crystals start to form with the condensation of liquid phase. Therefore, the macrostructure model of sinter can be divided into two parts, the melt zone and unfused ores, which is composed of the melt bonding the unfused ores together (as shown in Fig.5).

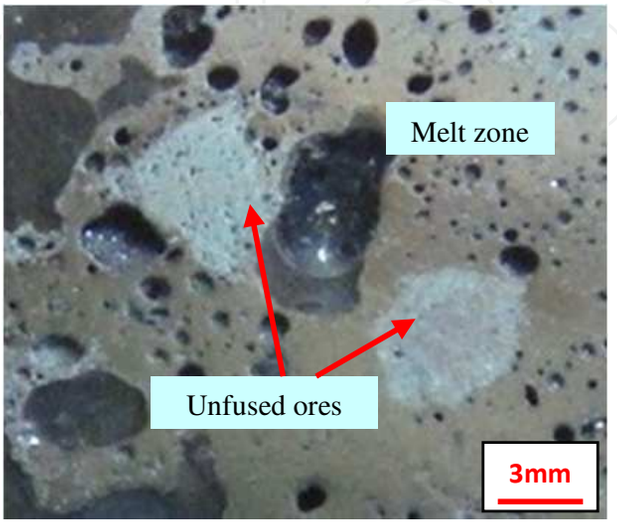

Figure 5. The structure of sinter

3.2. Microstructure of sinter

The microstructures of sinter were studied (Fig.6). The minerals in unfused ores are relatively simple, mainly for iron oxides, and its structure is relatively dense. Melt zone as the product of liquid condensing and crystallization, a variety of substances are precipitated during cooling process, and holes formed due to the shrinkage of liquid phase.

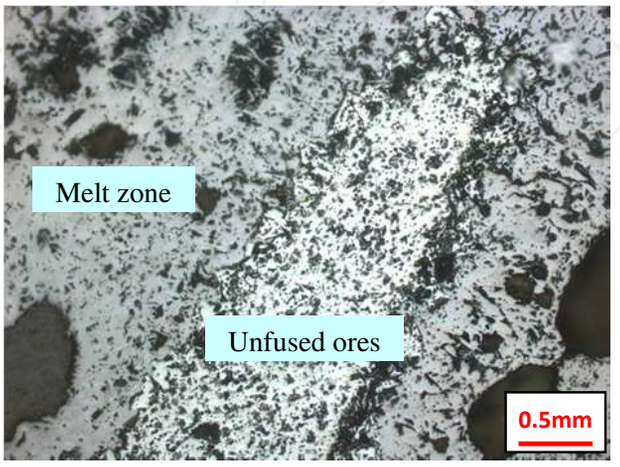

Figure 6. The Microstructure structure of sinter

http://dx.doi.org/10.5772/59659

The microstructures of melt zone are mainly divided into 3 kinds, corrosion structure of magnetite and CF, eutectic structure of CF and silicate, and pilotaxitic texture of hematite and CF, as shown in Fig.7. It's shown that the melt zone of sinter mainly presents as the corrosion structure of magnetite and calcium ferrite, which accounts for 80%-90% in melt zone. And a few partial areas rich in porosity present as mixed structure of hematite and calcium ferrite, or the eutectic structure of calcium ferrite and silicate. So, SFCA is the most important bonding phase in melt zone.

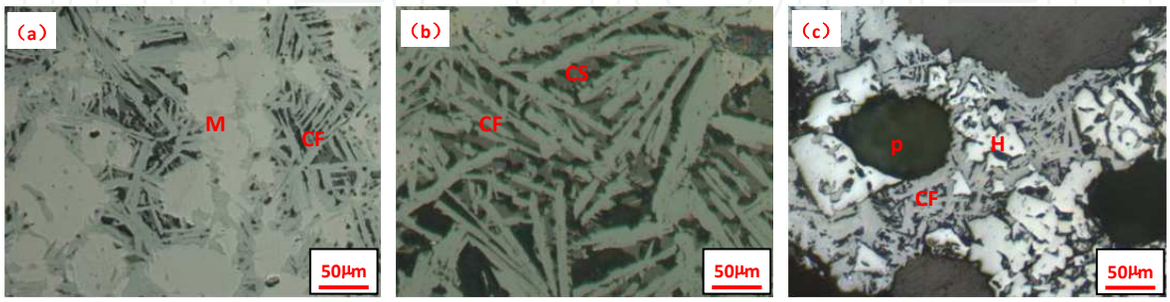

(a) corrosion structure of magnetite and CF, (b) eutectic structure of CF and silicate, (c) pilotaxitic texture of hematite and CF;H—hematite, M—magnetite, CF—calcium ferrite, CS—silicate, P—pole

Figure 7. Microstructures of melt zone

3.3. Morphology characteristics of calcium ferrite

According to the difference in the characteristics of calcium ferrite, they can be divided into four types of morphology, including plate-type, sheet-type, columnar-type, and acicular-type, which are shown in Fig.8. The chemical compositions of four kinds of calcium ferrite were studied, and the fracture toughness of different morphology of calcium ferrite was tested.

The results of energy spectrum analyses and fracture toughness tests for different types of SFCA are shown in Table 3. It can be seen that SFCA of acicular-type and columnar-type have lower Fe_2O_3 content than plate-type and granular-type, but higher contents of Ca and Si. There was no obvious difference in the content of Al_2O_3 among four structures, while SFCA of columnar& acicular-type has lower content of MgO than plate& sheet-type. The components of columnar-SFCA is closed to calcium diferrite ($\omega(CaO) = 14.9$), and acicular-SFCA has a relative component between calcium diferrite and the eutectic chemicals of $CaO \cdot Fe_2O_3$-$CaO \cdot Fe_2O_3$.

Fracture toughness was used to measure the microstrength of various types of SFCA. As shown in Table 3, the order of the strength of four kinds of SFCA is acicular-type>columnar-type>sheet-type>platy-type, while the strength of the sheet-type and plate-type are close, as well as the plate-type and sheet-type. Due to their similar strength, acicular-type and columnar-type are named as columnar&acicular-type, as well as the plate&sheet-type. The corrosion structure of magnetite and the columnar&acicular-type is the best microstructure with the highest strength.

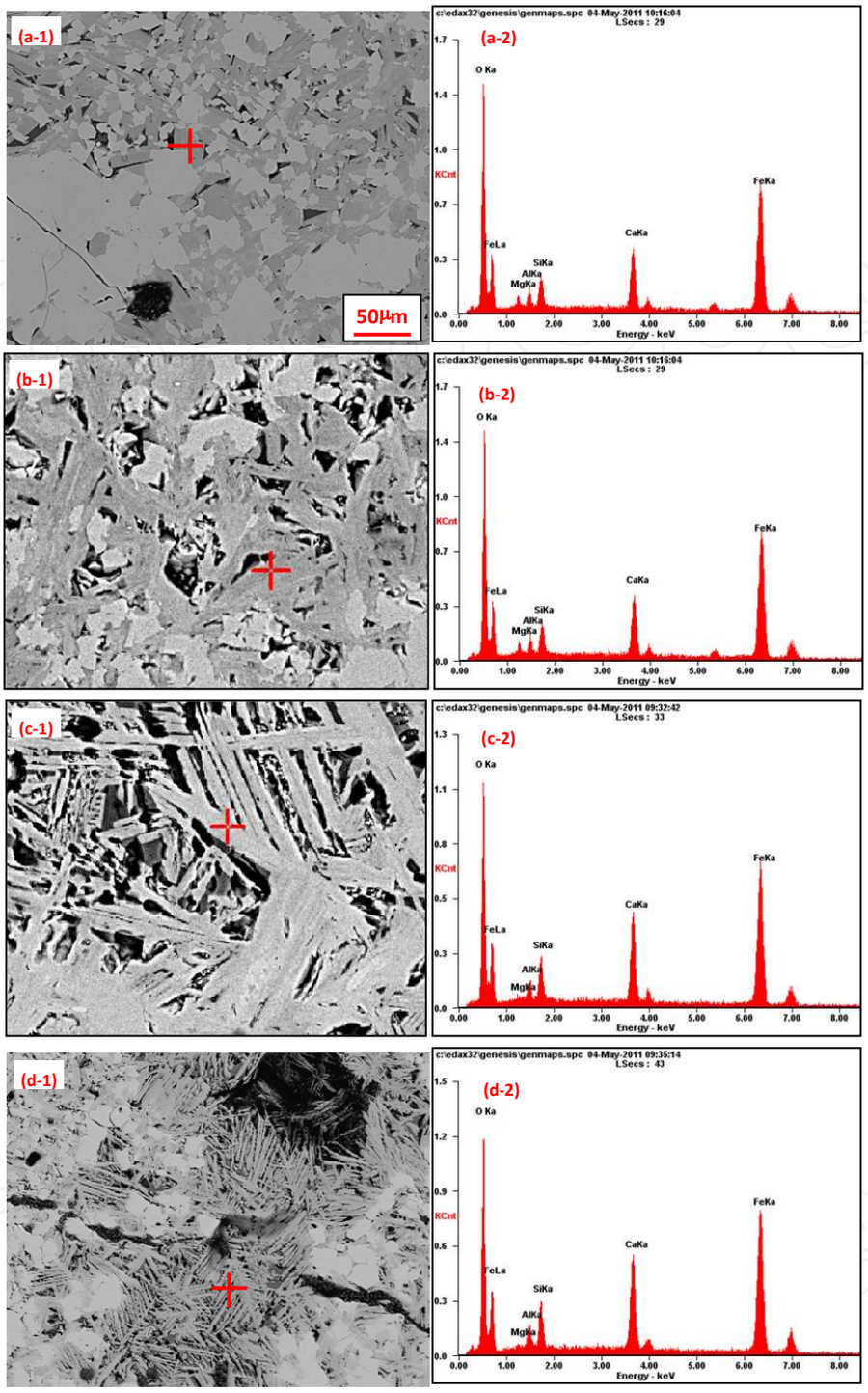

(a-1) Platy SFCA of SEM;(b-1) Sheet SFCA of SEM;(c-1) Columnar SFCA of SEM;(d-1) Acicular SFCA of SEM

(a-2) Platy SFCA of EDS;(b-2) Sheet SFCA of EDS;(c-2) Columnar SFCA of EDS;(d-2) Acicular SFCA of EDS

Figure 8. The structural morphology of SFCA

Consequently, increasing the content of liquid phase in melt zone and developing the bonding phase that is mainly composed by columnar&acicular-type SFCA seem to be effective measures to improve sinter strength.

http://dx.doi.org/10.5772/59659

Structure of SFCA	Fracture toughness / MPa·m^{-2}	Chemical component /%				
		CaO	Fe_2O_3	SiO_2	Al_2O_3	MgO
Platy-type	0.85	9.07-10.65	82.50-89.00	2.59-4.05	2.83-4.16	0.55-1.92
Sheet-type	0.91	10.75-12.49	71.79-85.66	3.73-6.66	3.03-4.11	0.92-2.28
Columnar-type	1.33	13.27-15.43	68.07-78.86	7.09-9.26	3.39-4.44	0.40-1.43
Acicular-type	1.39	13.99-17.04	70.57-75.37	6.60-9.99	3.20-4.25	0.57-0.80

Table 3. The component and fracture toughness of various SFCA

4. Crystal behavior of calcium ferrite during cooling process

4.1. Crystal behavior of calcium ferrite at different temperature

Calcium oxide (mass fraction 8%) was added into iron ores to ensure the formation of CF melt during sintering. Briquettes were cooled down to 1280℃, 1250℃, 1200℃, 1150℃, and 1050℃ at a cooling rate of 50℃/min respectively, and then quenched by water. Fig.9 shows the micrograph of products at different quenching temperature.

Dominated mineral composition were hematite and CF in each products, and microstructure was corrading, however the crystallization had obvious differences (Table 4).

According to the results, we preliminary deduce that the precipitation temperature of crystal in CF system is close to 1200℃.In order to verify this inference, briquettes were cooled with 50 ℃/min to 1200 ℃, and holding 10 min at this temperature, then quenched by water finally. It was found experimentally that as the holding time prolonged, crystalline morphology became significant needle-like. Although dominated mineral compositions were hematite and CF, precipitation quantity of CF increased.

Quenching temperature	Micrograph	Mineral composition and microstructure
1280℃ 1250℃	Fig. 1a Fig. 1b	No crystalline state were formed. The binder phase, which had no time to crystallize under high temperature quenching, keeped the original morphology.
1200℃	Fig. 1c	The rudiment of the crystalline state CF was obtained, and its characteristic of morphology was unidirectional extension.
1150℃ 1050℃	Fig. 1d Fig. 1e	Melt were crystallized gradually, developed more fully, in addition, needle-like CF were precipitated.

Table 4. Mineral composition and microstructure of different quenching temperature

Undercooling is a essential driving force for phase transition. When the temperature is lower than the melting point, undercooling $\triangle T$($\triangle T$=T_m-T, T_m—melting temperature, T—actual

temperature) is obtained. It was found by spectrum, the component of CF was close to the eutectic point of Fe_2O_3–CaO system. Fig. 10 [5]shows the temperature of melt precipitation nearby eutectic point was just higher than 1200 ℃, and the crystal had undercooling condition at this temperature.It also proved the conclusion that CF,which precipitated at about 1200℃, had good crystallization capacity. The crystal precipitation process was closed to the equilibrium state.

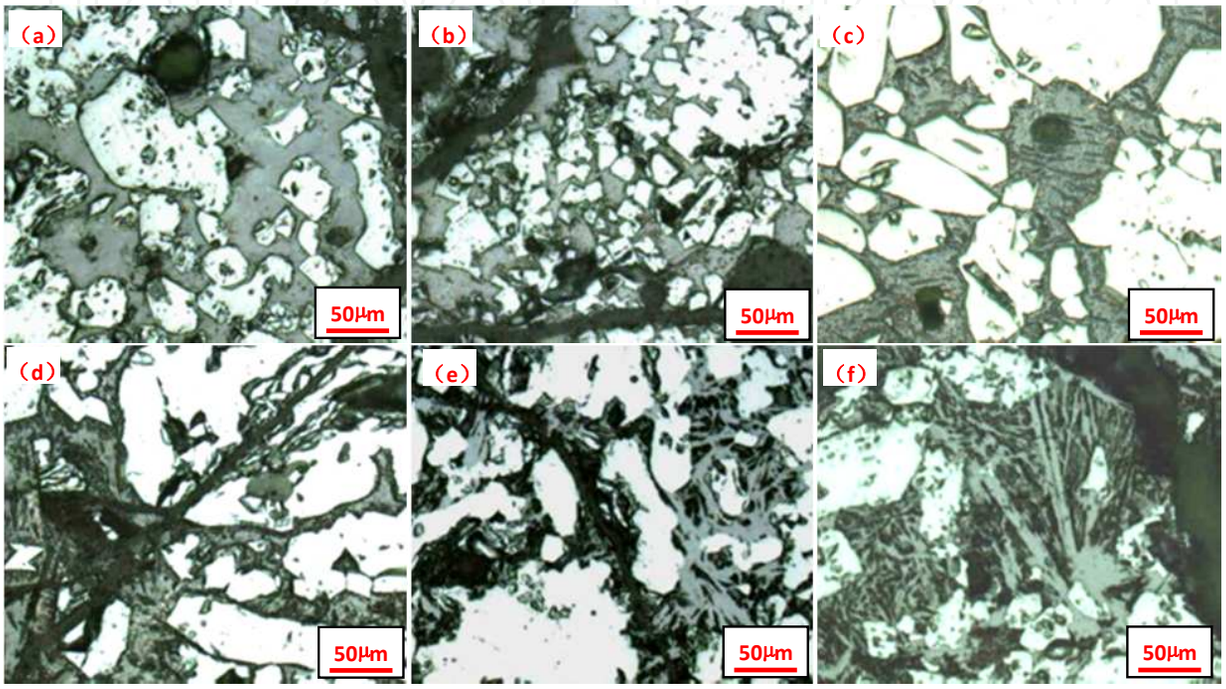

(a) 1280℃; (b) 1250℃; (c) 1200℃; (d) 1150℃
(e) 1050℃; (f) Holding 10 min at 1200℃
White—Hematite, Gray—CF, Black—Void

Figure 9. Micrograph of different quenching temperature

In addition, we can find that the rudiment of CF was excessive and small, and exhibited unidirectional extension, which would become needle-liked when it developed. All of these conform to the morphology features of rapid crystallization, which proved that CF crystal had rapid growth speed, strong crystal ability, and little affection by dynamics and extenal factors.

4.2. Effect of the cooling rate on crystallization of calcium ferrite

Cooling rate determines the time of crystal precipitation, which is one of important factors of crystallization. Using controllable cooling design, cooling rate was controled at 150℃/min, 100℃/min, 50℃/min in high temperature stage (≥1000℃), and 50℃/min in low temperature stage (≤ 1000℃). Natural cooling method was adopted when briquettes was cooled down to 600℃.

http://dx.doi.org/10.5772/59659

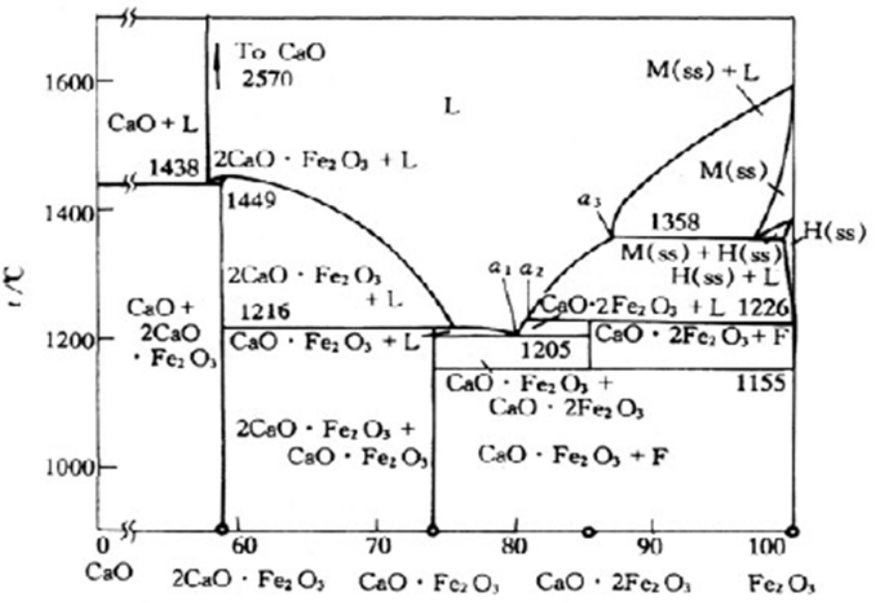

L—Liquid;F—Hematite;M(ss)—Magnetite solid solution;H(ss) —Hematite solid solution

Figure 10. Binary phase diagram of CaO and Fe_2O_3 [17,18]

Adding 8% of calcium oxide(R=2.3) into raw material as flux. After sintering and cooling, Fig. 11 and Table 5 provides a set of typical microstructure corresponding to the samples prepared from different cooling rate.

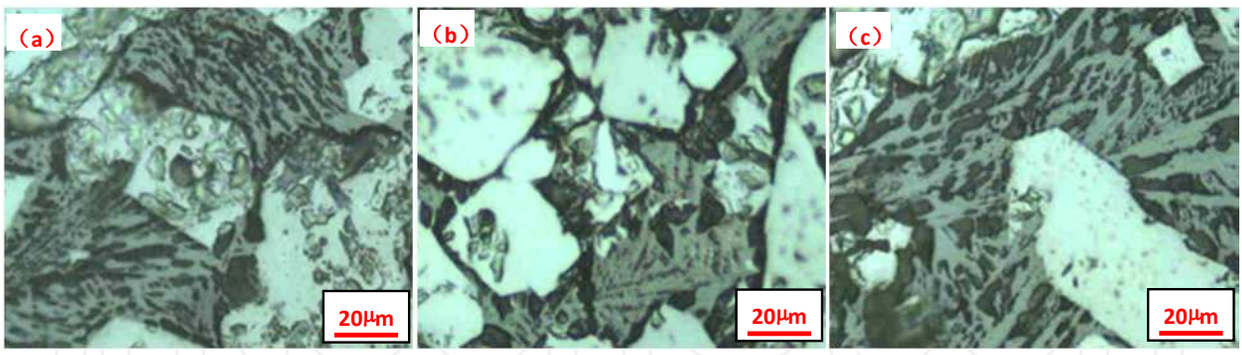

(a) 150℃/min；(b) 100℃/min ；(c) 50℃/min

White—Hematite，Gray—CF，Black—Void

Figure 11. Micrograph of different cooling rate

Based on the experimental results, it was said that CF crystal can precipitate in rapid cooling rate. At the same time, slowing cooling rate was significantly in favour of further development of the crystal.

In the actual production process, cooling rate of the upper and lower material layers are 120~130℃/min and 40~50℃/min respectively [6]. During the production of high-basicity sinter, we can deduce that the cooling process of lower material layer is relative slow, and this can be in favor of the crystallization of needle-like CF and development of melting structure. From the perspective of crystal precipitation behavior, we conclude that the lower material layer is superior to upper one.

Cooling rate	Micrograph	Mineral composition and microstructure
150℃/min	Fig. 3a	Crystal rudiment of CF was found, which further confirmed that CF had strong crystalize abiliity.
100℃/min	Fig. 3b	The crystal precipitation became obvious with decreasing cooling rate, and crystal tended to intensive.
50℃/min	Fig. 3c	Along with melt crystallizing fully, CF developed to needle-like morphology, which formed interlaced and corrasive structrue with hematite.

Table 5. Mineral composition and microstructure of different cooling rate

5. Effect of chemical compositions on crystallization of calcium ferrite

The influences of Ca/Fe, SiO_2, Al_2O_3 and MgO on the generation of calcium ferrite in melt zone were studied. The molar ratio of Ca/Fe and the content of MgO were changed by adding calcium or magnesium fluxes, and the contents of SiO_2 and Al_2O_3 were changed by regulating the types of iron ores used.

5.1. Ca/Fe in melt zone

The influences of Ca/Fe on the generation of columnar&acicular-SFCA in melt zone were studied. The results are shown in Fig.12. As the molar ration of Ca/Fe is low, there is little columnar&acicular-SFCA in melt zone. With the increase of Ca/Fe, the generation of SFCA is improved first, then down when the Ca/Fe exceeds 0.4.

The influence of Ca/Fe on the microstructure of melt zone is shown in Fig.10. The total content of SFCA increases with the improvement of the molar ratio of Ca/Fe, but columnar&acicular-SFCA increases first and then decreases. When Ca/Fe is 0.23, the morphology of SFCA is mainly platy-type(Fig.13(a)). As Ca/Fe reaches to 0.3-0.4, the main form of SFCA exists as columnar&acicular-type, which reaches the maximum amount (Fig.13(c) ~ Fig.13(e)). When Ca/Fe increases to 0.5, the content of columnar&acicular-SFCA decreases instead, and sheet-type SFCA of interconnection mode forms remarkably (Fig.13(f)).

http://dx.doi.org/10.5772/59659

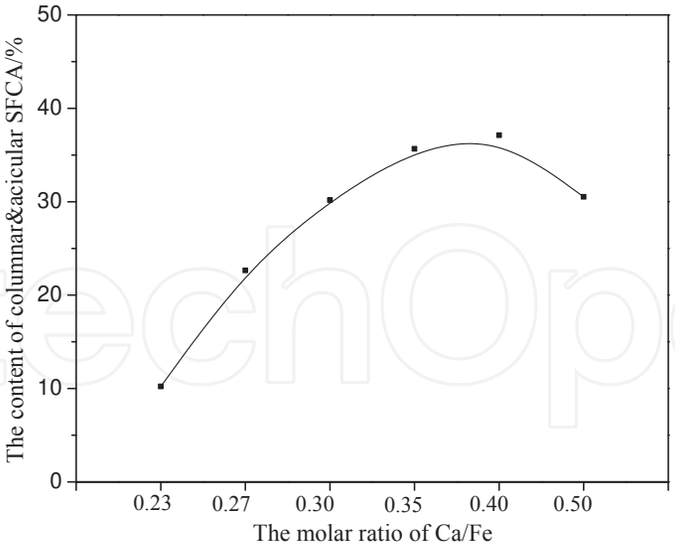

Figure 12. Influence of Ca/Fe on the generation of SFCA in melt zone

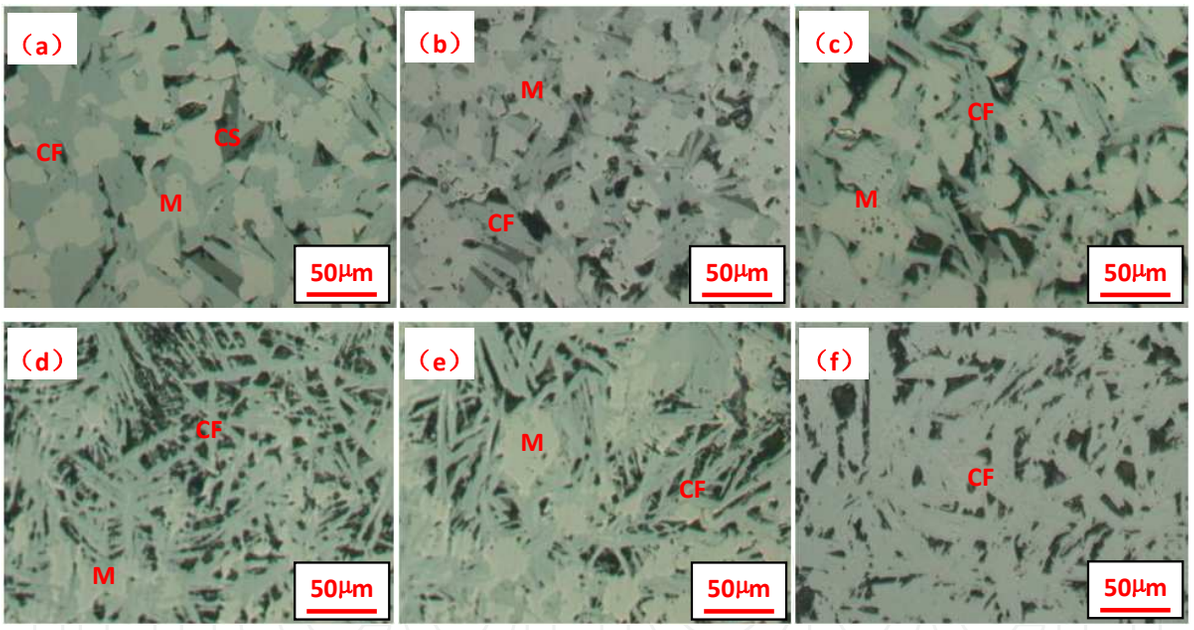

(a) Ca/Fe=0.23；(b) Ca/Fe=0.27；(c) Ca/Fe=0.30

(d) Ca/Fe =0.35；(e) Ca/Fe =0.40；(f) Ca/Fe =0.50

M—Magnetite，SFCA—Calcium ferrite，CS—Silicate

Figure 13. Influence of Ca/Fe on the microstructure of melt zone

5.2. SiO_2 content in melt zone

The influences of SiO_2 content in melt zone on the generation of columnar&acicular-SFCA and the microstructure were studied. The results are shown in Fig.14 and Fig.15.

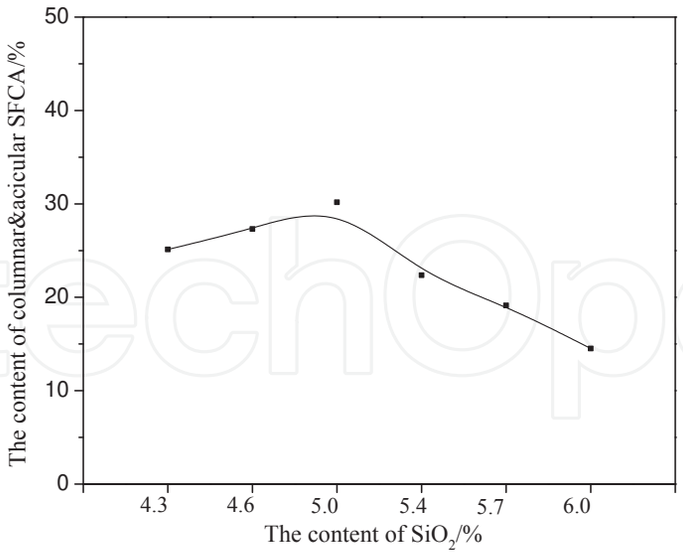

Figure 14. Influence of SiO_2 on the generation of SFCA in melt zone

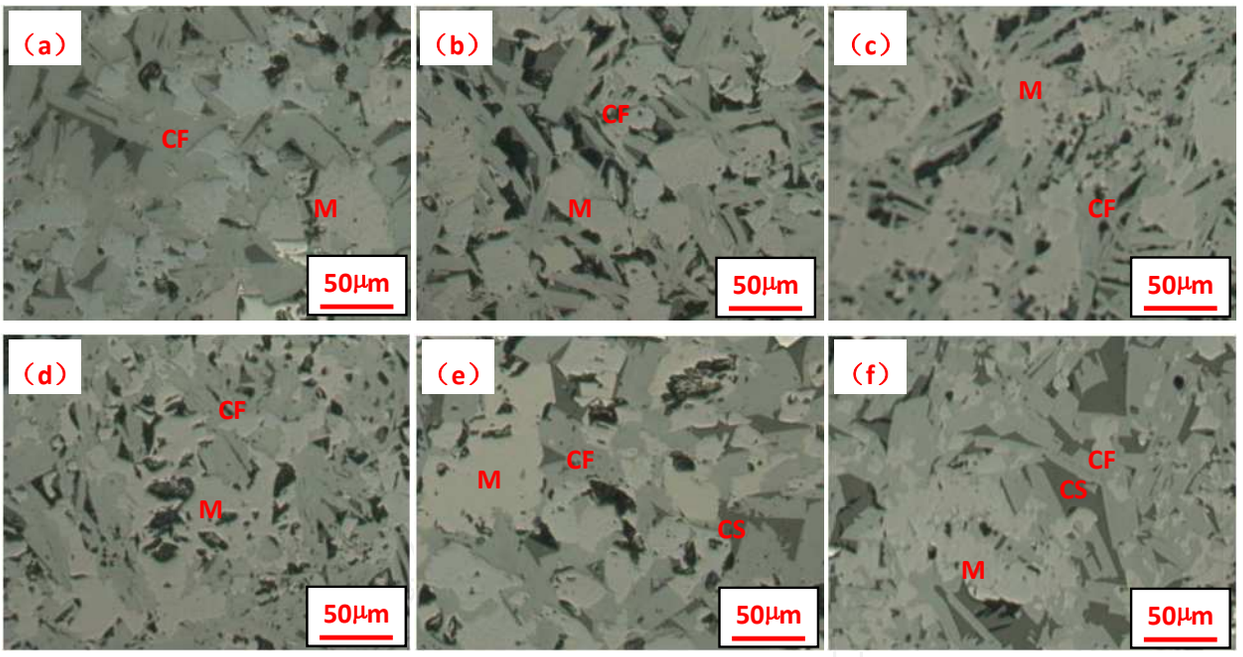

(a) $SiO_2$4.3%; (b) $SiO_2$4.6%; (c) $SiO_2$5.0%; (d) $SiO_2$5. 4%; (e) $SiO_2$5.7%; (f) $SiO_2$6.0%

M—Magnetite, SFCA—Calcium ferrite, CS—Silicate

Figure 15. Influence of SiO_2 on the microstructure of melt zone

For the influence of SiO_2, when the content of SiO_2 increases from 4.3% to 5.0%, the content of columnar&acicular-SFCA increases to some extent (Fig.15(a) ~ Fig.15 (c)). SiO_2 content of 5.0% would benefit the generation of columnar&acicular-SFCA because SiO_2 is an important ingredient for SFCA formation. While SiO_2 exceeds 5.0%, the reaction between CaO and SiO_2

http://dx.doi.org/10.5772/59659

occurs more easily than that between CaO and Fe_2O_3. As a consequence, the amount of SFCA coming from the reaction between CaO and Fe_2O_3 is reduced. And it facilitates producing platy SFCA other than columnar&acicular-type since more silicate is generated (Fig.15(e) and Fig. 15(f)).

5.3. Al_2O_3 content in melt zone

Al_2O_3 is also an influencing factor for SFCA [19]. The effect of Al_2O_3 on the generation of SFCA in melt zone is investigated, and the results are shown in Fig.16. When the content of Al_2O_3 is not more than 1.8%, columnar&acicular-SFCA generates sufficiently. As Al_2O_3 content continues to increase, it's disadvantage for the form of columnar&acicular-SFCA.

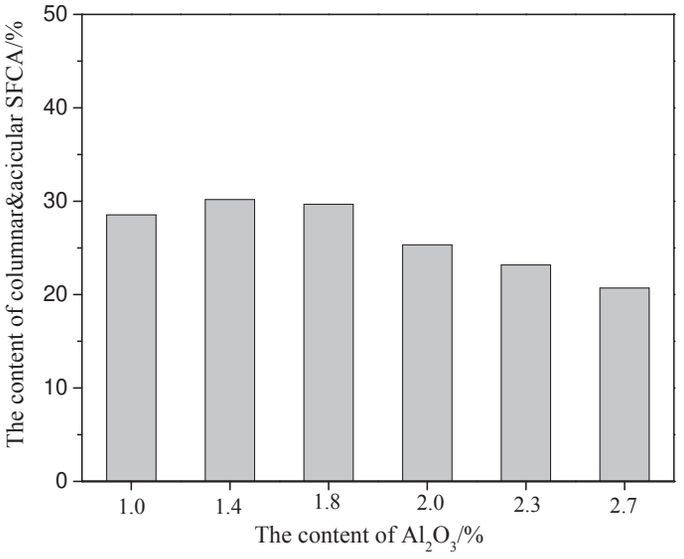

Figure 16. Influence of Al_2O_3 on the generation of SFCA in melt zone

The influence of Al_2O_3 on the microstructure of melt zone is presented in Fig.10. When the content of Al_2O_3 is under 1.8%, melt zone mainly consists of the corrosion structure formed by SFCA and magnetite(Fig.17(a)~ (Fig.17(c)). But the microstructure would change markedly when the content of Al_2O_3 is more than 1.8%. The columnar&acicular-SFCA is suppressed and the platy SFCA gets developed (Fig.17(d)~ (Fig.17(f))). When the content of Al_2O_3 is excessively high, it would not only increase the melting point of sintering mix, but also increase the viscosity of liquid phase. Thus the fluidity of liquid phase is worsened, which makes it difficult for the precipitation of columnar&acicular-SFCA that crystallises along one-way extension, and makes the size and quantity of the pores in the melt zone increase.

5.4. MgO content in melt zone

In the same way, the influence of MgO on the formation of SFCA was researched. With the increase of the content of MgO, the content of SFCA decreases(as shown in Fig.18). And the main reason is that Mg^{2+} entered into the crystal lattice of magnetite, forming magnesiaspinel

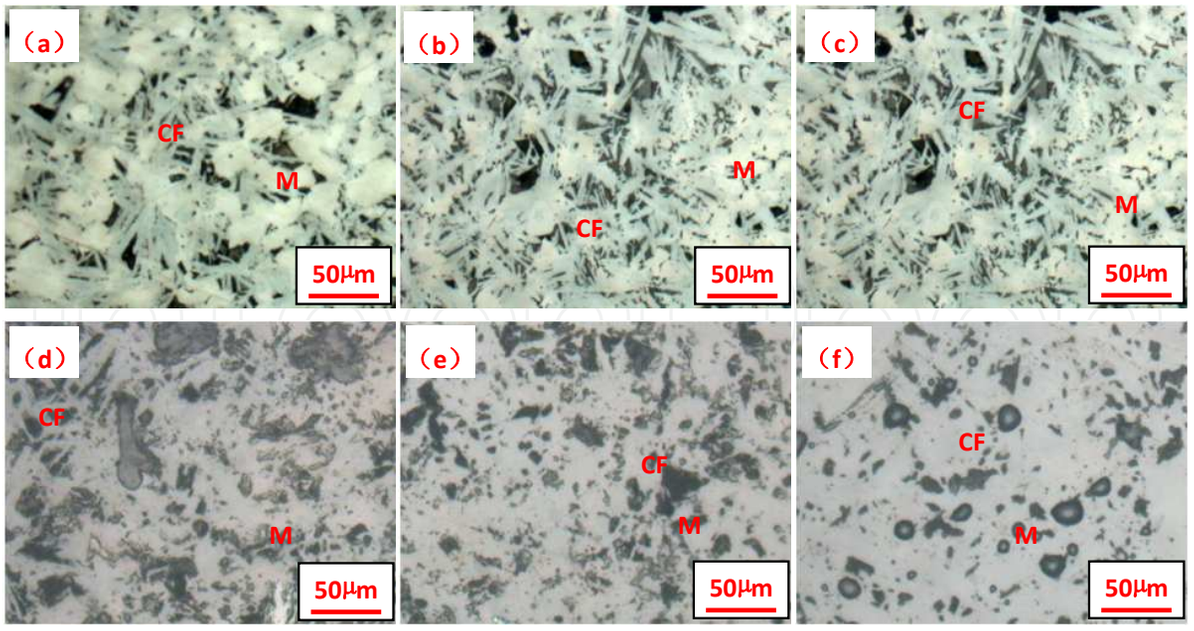

(a) $Al_2O_3$1.0%; (b) $Al_2O_3$1.4%; (c) $Al_2O_3$1.8%
(d) $Al_2O_3$2.0%; (e) $Al_2O_3$2.2%; (f) $Al_2O_3$2.6%

Figure 17. Influence of Al_2O_3 on the microstructure of melt zone

[(Fe,Mg) O Fe_2O_3]. The crystal lattice of magnetite is stabilised by solid solution of Mg^{2+}. As a result, it would suppress the formation of SFCA by preventing the oxidising reaction from magnetite to hematite [20,21]. With the increase of MgO from 1.4% to 6.4%, the content of columnar&acicular-SFCA decreases from 34.67% to 18.17%.

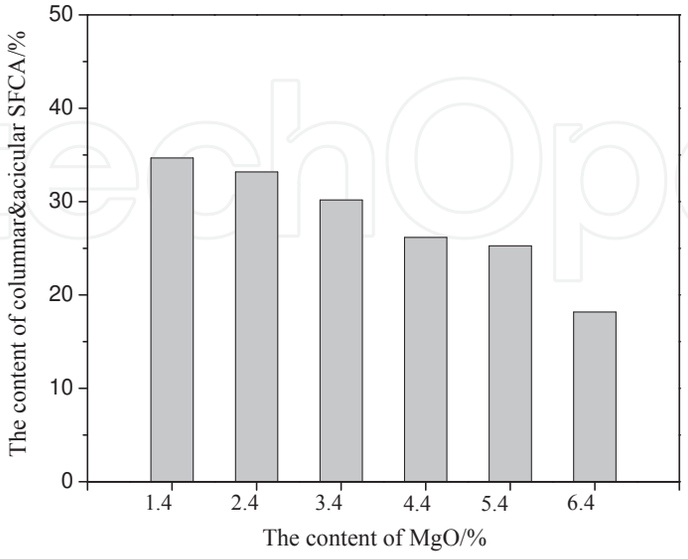

Figure 18. Influence of MgO on the generation of SFCA in melt zone

http://dx.doi.org/10.5772/59659

The influence of MgO on the microstructure of melt zone is shown in Fig.19. When the content of MgO is excessively high, lumpy pieces of recrystallisation magnetite are generated in melt zone, and the content of columnar&acicular-SFCA is decreased significantly.

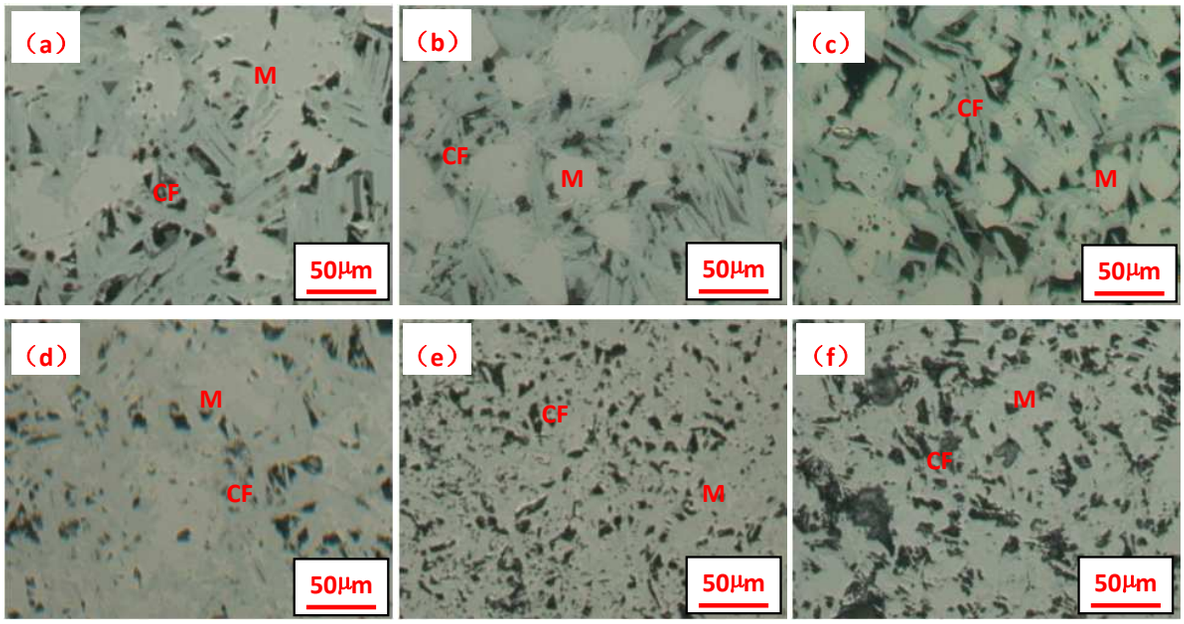

(a) MgO1.4%; (b) MgO2.4%; (c) MgO3.4%
(d) MgO4.4%; (e) MgO5.4%; (f) MgO6.4%

Figure 19. Influence of MgO on the microstructure of melt zone

5.5. Methods of optimising SFCA generation

Therefore, the chemical composition of melt zone plays a considerably important role in liquid phase and the generation of SFCA. The suitable chemical components of melt zone have been proved to be that, the molar ratio of Ca/Fe is 0.3-0.4, the content of SiO_2 is about 5%, the content of Al_2O_3 is less than 1.8%, the content of MgO should be controlled as low as possible under the condition guaranteeing the slag-making of blast furnace. In accordance with the principles introduced above (Table 6), the performance of mixtures on the mineralization can be optimised.

Ca/Fe(molar ratio)	SiO_2 content/%	Al_2O_3 content/%	MgO content/%
0.3-0.4	about 5.0%	≤1.8	Low as possible

Table 6. Suitable ranges of chemical component in melt zone for mineralization

The chemical composition of melt zone can be calculated by Equation 1. On the basis of that, all of the fluxes react with the fine iron ores less than 0.5mm to form the melt zone. According

to the equation, as knowing the composition of raw materials, adhesive fines (-0.5mm) content and the proportions of raw materials, the chemical compositions in melt zone can be figured out.

$$w(Q) = \frac{\sum x_i \cdot x_i^{-0.5} \cdot w_i^Q + \sum x_j \cdot w_j^Q}{(\sum x_i \cdot x_i^{-0.5} + \sum x_j)(1 - \sum x_i \cdot x_i^{-0.5} \cdot w_i^{LOI} - \sum x_j \cdot w_j^{LOI})} \quad (1)$$

Where w(Q) is the content of chemical composition Q in melt zone, %;

x_i is the ratio of iron ore i in the mixture, %;

$x_i^{-0.5}$ is the content of fine grains(-0.5mm) in ore i, %;

w_i^Q is the content of chemical composition Q in adhesive fines(-0.5mm) of ore i, %;

w_i^{LOI} is the loss on ignition of fraction -0.5mm in ore i, %;

x_j is the ratio of flux j in the mixture, %;

w_j^Q is the content of chemical composition Q in flux j, %;

w_j^{LOI} is the loss on ignition of flux j,%.

Take a sintering plant in china as an example. The basic ore blending scheme is the producing plan before optimizing. The chemical composition in melt zone of basic scheme is shown in Table 7. According the suitable ranges of relative components, the molar ratio of Ca/Fe and the contents of SiO_2, Al_2O_3 are all beyond their appropriate values in basic scheme. Columnar&acicular-SFCA are low because the chemical component of melt zone fails to meet the expected match.

Scheme	Chemical component of melt zone				Content of C.&A.-SFCA/%
Molar ratio of Ca/Fe	SiO2 /%	Al_2O3 /%	MgO /%		
Basic	0.28	5.43	2.03	2.98	23.86
Optimization A	0.32	5.08	1.78	3.08	32.66
Optimization B	0.33	5.16	1.82	3.14	34.27

Table 7. The chemical component of melt zone and the property of mineralisation

In order to optimise the chemical components of melt zone, it is necessary to increase the molar ratio of Ca/Fe and reduce the contents of Al_2O_3 and SiO_2 in the fraction of -0.5mm on the basis of basic scheme. The methods of optimisation are decreasing the content of -0.5mm in blending ores to raise the Ca/Fe, and decreasing the ores of high Al_2O_3 and SiO_2. Two ore blending schemes of optimisation are obtained. The chemical components of melt zone are shown in

http://dx.doi.org/10.5772/59659

Table 7 after optimising the ore blending. It can be seen that the molar ratio of Ca/Fe of Optimisation A and Optimisation B increased to 0.32 and 0.33 respectively, the content of SiO_2 decreased to 5.08% and 5.16%, and Al_2O_3 decreased to 1.78% and 1.82%, all reaching or approaching the suitable range for mineralisation. Compared with the basic scheme.

The influences of mineralisation improvement by optimising the ore blending on sintering are shown in Table 8. When the proportion of coke breeze remained at 5%, sintering speed of two optimising schemes increases from 21.94mm/min to 23.55mm/min, 23.78mm/min, the yield increases from 72.66 to 74.05%, 73.69%, the productivity increases from 1.48t/(m^2 h) to 1.60t/(m^2 h), 1.59t/(m^2 h), and the tumbler strength increases from 65.00% to 66.40%, 66.45%. When the production and quality indexes are comparative, the ratio of coke breeze can be decreased from 5.0% to 4.7%, and the solid fuel consumption reduces by 5.6%.

Scheme	Ratio of coke breeze/%	Sintering speed /mm·min^{-1}	Yield/%	Tumbler index/%	Productivity /t·m^{-2}·h^{-1}
Standard	5.0	21.94	72.66	65.00	1.48
Optimization A	5.0	23.55	74.05	66.74	1.60
Optimization A	4.7	22.22	71.88	64.56	1.48
Optimization B	5.0	23.78	73.69	66.45	1.59

Table 8. The influence of the optimisation of mineralisation to the sintering

6. Conclusions

1. The structure of sinter composes of a melt zone and unfused ores. Sinter strength is mainly subjected to the properties of melt zone since unfused ores are wrapped by melt zone is proposed. It facilitates obtaining sinter of high strength with the increase of SFCA in melt zone during melt condensation.
2. Crystalline CF began to precipitate at about 1200℃.The lower cooling temperature, the better crystal growth, and the more content of precipitated needle-like CF. CF crystal has rapid growing speed, strong crystal ability, and little affection by dynamics and external factors. However, slowdowning the cooling rate is obviously favorable to development of crystal.
3. SFCA can be divided into four structural types, including plate-type, sheet-type, columnar-type, and acicular-type. The strength of columnar&acicular-type SFCA is better than that of plate& sheet-type.
4. The suitable chemical components for mineralisation of the melt zone are that, the molar ratio of Ca/Fe is 0.3-0.4, the content of SiO_2 is about 5%, the content of Al_2O_3 is less than 1.8%, and the content of MgO should be controlled as low as possible for guaranteeing the slag-making of blast furnace.

Acknowledgements

The authors are grateful to the National Natural Science Foundation of China(no. 51304245) and the Postdoctoral Science Foundation (no.2013M540639 and no.2014T70691) for supporting this research.

Author details

Min Gan, Xiaohui Fan* and Xuling Chen

*Address all correspondence to: 156703017@qq.com

Department of Ferrous Metallurgy, Central South University Changsha, Hunan, China

References

[1] M.J.Cumming, and J.A.Thurlby. Developments in the modelling and simulation of iron ore sintering, *Ironmaking & Steelmaking*, 1990, 17 (4), 245-254.

[2] D.F.Ball. Agglomeration of iron ores, 1973, Heinemann Educational.

[3] P.R.Dawson. Recent developments in iron ore sintering, *Ironmaking & Steelmaking*, 1993, 20 (2), 135-143.

[4] M.I.Pownceby and J. M. F.Clout. Importance of Fine Ore Chemical Composition and High Temperature Phase Relations: Applications to Iron Ore Sintering and Pelletising. Mineral Processing and Extractive Metallurgy: Transactions of the Institute of Mining and Metallurgy, Section C, 2003, 112(1), 44-51.

[5] X.H.Fan,J.Meng,X.L.Chen,J.M.Zhuang,Y.Li,and L.S.Yuan. Influence Factors of Calcium Ferrite Formation in Iron Ore Sintering, Journal of Central South University, 2008, 36, (6),1125-1131. (in Chinese)

[6] T.Miyashita, N.Sakamoto, and Hiroshi Fukuyo. Influence of Mineral Structure on Sinter Agglomerate's Propeties, Trans ISIJ, 1982, 22(7), B-199.

[7] Y.Ishikawa. Improvement of Sinter Quality Based on the Mineralogical Propeties of Ores, Ironmaking Proc, 1983,42,17-29.

[8] X.R.Liu,G.Z.Qiu,R.Z.Cai,and S.F.Lin. The Mineralogy Research on the Ferrite of Low-temperature Sintering, Sintering and Pelletizing, 2000, 25 (2),7-10. (in Chinese)

[9] A.Cores, A.Babich, M.Muniz, S.Ferreira and J.Mochon.The Influence of Different Iron Ores Mixtures Composition on the Quality of Sinter. ISIJ International, 2010, 50(8), 1089-1098.

[10] L.H. Hsieh and J.A.Whiterman. Sintering conditions for simulating the formation of mineral phases in industrial iron ore sinter, *ISIJ Int.*, 1989, 29 (1), 24-32.

[11] C.E.Loo, R.P. Williarns and L.T. Mattews. Designing iron ore sinter mixes for optimum raw material utilization, Proceeding of The Six International Iron & Steel Congress, 1990, Nagoya, the Iron and Steel Institute of Japan.

[12] H.G.Li, J.L.Zhang, Y.D.Pei, Z.X.Zhao and Z.J.Ma. Melting characteristics of iron ore fine during sintering process, *J. Iron Steel Res. Int.*, 2011, 18, (5), 11-15.

[13] O.Iun, H.Kenichi, H.Yohozoh and K.Shinagawa, Influence of iron ore characteristics on penetrating behavior of melt into layer, *ISIJ Int.*, 2003, 43 (9), 1384-1392.

[14] X.H.Fan. Principle and technology of iron ore matching for sintering, 2013, 39-42, Beijing, Metallurgical industry press. (in Chinese)

[15] G. S.Feng, S. L.Wu, H. L.Han, L.W.Ma and W. Z.Jiang. Sintering Characteristics of Fluxes and Their Structure Optimization. International Journal of Minerals Metallurgy and Materials, 2011, 18(03): 270-276.

[16] M.Gan: Fundamental Research on Iron Ore Sintering with Biomass Energy, Doctor Dissertation, (2012), 85. (in Chinese)

[17] P.Bert, M.Arnulf. Phase Equilibria in the System CaO-Iron Oxide in Air and at 1 Atm. O_2 Pressure. Journal of The American Ceramic Society, 1958, 41(11), 445-454

[18] J. W.Jeon, S.M.Jung and Y.Sasaki. Formation of Calcium Ferrites under Controlled Oxygen. ISIJ International, 2010, 50(8), 1064-1070.

[19] L.Lu, R. J.Holmes and J. R. Manuel, Effects of alumina on Sintering Performance of Hematite Iron Ores. ISIJ International, 2007, 47(3), 349-358.

[20] H. S.Kim, J. H.Park and Y. C.Cho. Crystal Structure of Calcium and Aluminium Silicoferrite in Iron Ore Sinter. Ironmaking & Steelmaking, 2002, 29(4), 266-270.

[21] K.Yajima, and S. M.Jung. Data Arrangement and Consideration of Evaluation Standard for Silico-Ferrite of Calcium and Alminum (SFCA) Phase in Sintering Process. ISIJ International, 2012, 52(3), 535-537.

IntechOpen